AIAA Guidance, Navigation, and Control Conference and Exhibit
5-8 August 2002, Monterey, California

AIAA 2002-5030

Tracking and pointing of target by a Bifocal Relay Mirror Spacecraft using attitude control and fast steering mirrors tilting

Marcello Romano and Brij N. Agrawal

Spacecraft Research and Design Center
Naval Postgraduate School, Monterey, CA 93943

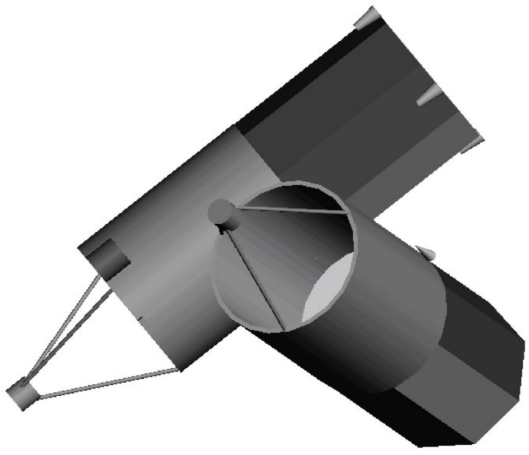

Guidance, Navigation, and Control Conference and Exhibit
August 5–8, 2002/Monterey, CA

Tracking and pointing of target by a Bifocal Relay Mirror Spacecraft using attitude control and fast steering mirrors tilting

Marcello Romano* and Brij N. Agrawal†

Spacecraft Research and Design Center
Naval Postgraduate School, Monterey, CA 93943

The present paper reports the results of numerical simulations carried out on a model of the Bifocal Relay Mirror spacecraft. This spacecraft consists of two large mechanically and optically coupled telescopes, used to redirect a laser beam from a ground-based, airborne or spacecraft based source to a distant target point on the earth or in space. The two telescopes are gimbaled and the spacecraft inertia has a large variation during the angle maneuvers needed to maintain the laser cross link. Moreover the spacecraft has very tight pointing and jitter requirements. The task of the presented simulations was to preliminarily validate and compare two different control approaches proposed for the tracking and pointing of the target of the Bifocal Relay Mirror. The attitude control system consists of reaction wheels, star trackers and rate gyros. The optical control system consists of two two-axis fast steering mirrors and two optical tracker sensors. In the first control option considered, feed-forward and PD feedback are used for the spacecraft attitude control, while PID feedback is used for the optical subsystem, in order to compensate the pointing error. In the second control approach, the spacecraft and the optical control systems are integrated.

Nomenclature

$\underline{h}$	Angular momentum vector
$\underline{T}$	Torque vector
$\underline{I}$	Moment of inertia dyadic
$\underline{\omega}$	Angular velocity vector
x, y, z	Cartesian axes coordinates
O	Cartesian axes origin
i, k	Indexes
β	Relative angle of a mirror with respect to its base
ξ	Damping ratio
ω_n	Natural frequency
t	Internal torque
$\underline{i}$	Versor
j	Moment of inertia

A Subscripts

$S, S/C$	Spacecraft
R	Receiver portion of the spacecraft
T	Transmitter portion of the spacecraft
w	Reaction wheel
m	Mirror
rel	Relative

B Acronyms

BRM	Bifocal Relay Mirror
d.o.f.	Degree of freedom
IRU	Inertial Reference Unit
FSM	Fast Steering Mirror
LOS	Line of sight
FF	Feed-Forward

I Introduction

MANY of the near future space missions will require high accuracy pointing and tracking of multiple targets at the same time. Applications include optical communications relay link satellites, laser sensors for formation flying fleets of space probes and several other civil and military uses. Optical frequencies provide extremely high antenna gain for relatively small antenna size, thereby allowing cross links to be closed with relatively low transmitter power and small terminals. Moreover, in case of relay satellite, the laser sources are on the grounds

*Ph.D., US National Research Council Associate Fellow. AIAA member.

†Professor and Director. AIAA Associate Fellow.

and that allow for relatively easy interchanging of lasers having different power or wavelengths for different type of utilization of the cross link.

However, the extremely narrow beam-width poses severe pointing, acquisition and tracking requirements.[1]

The Spacecraft Research and Design Center of Naval Postgraduate School participated in the Bifocal Relay Mirror (BRM) project, aiming to the preliminary study of a laser relay spacecraft for non-weapon military applications of laser links.

A Relay Mirror space application is an application of increased difficulty with respect to the typical spacebased telescopes application. In fact beyond a high line of sight stabilization capability it requires also the capability of line of site rate tracking. Moreover the foreseen Bifocal Relay Mirror Spacecraft application is still more challenging than the Relay Mirror Experiment described in ref.[2] In fact, while that experiment used both cooperative source and target (that is, both source and target were sending a beacon beam to the relay mirror spacecraft, allowing a closed loop pointing control) the Bifocal Relay Mirror Spacecraft is required to work with uncooperative targets.

The Bifocal Relay Mirror spacecraft is composed of two optically coupled telescopes and is used to redirect the laser light from ground-based, airborne or spacecraft based laser sources to distant target points on the earth or in space. The receiver telescope captures the incoming energy from the laser source, while a separate transmitter telescope, movable with respect to the other telescope, directs the laser beam at the desired target.

The preliminary design of the BRM Spacecraft was carried out by students of Naval Postgraduate School under a spacecraft design course. The transmitter and receiver telescopes have Cassegrain configuration with primary mirror of 1.64 meter diameter, and are gimbaled around a single axis. The transmitter telescope has the majority of the spacecraft bus subsystems, including the attitude control sensors and actuators. The spacecraft mass is $3300\,kg$ at launch and the spacecraft orbit altitude is $715\,km$ with an inclination of $40\,degrees$. The mission requirements are for a $3\,meters$ spot beam on the ground, beam jitter less than $144\,nano-radians$ and mean dwell duration per pass of $250\,seconds$. The spacecraft has three primary operational modes: sun bath, acquisition, and tracking. During the sun bath mode, non-operating period, the solar cell surfaces of the telescopes are kept normal to the sun axis to maximize the electric power output. During the acquisition mode, both source and target points are acquired, and then pointed and tracked for the duration of the dwell. The acquisition sequence consists of pitch and roll motion of transmitter telescope to acquire the target point. The yaw motion of the transmitter telescope and the one axis motion of the receiver telescope is used to acquire the source point.

The preliminary design effort identified the need to develop several technologies to meet the mission requirements, especially in the area of fine acquisition, tracking, and pointing, and beam control optics. In particular there are several unique multibody pointing and tracking control problems in the Bifocal Relay Mirror spacecraft: in fact the motion of the two massive telescopes results in a continual change of the spacecraft inertia during the operation.

The present paper focuses on the problem of pointing and tracking of the target. In particular, the task of the research presented here was to perform preliminary simulations of the dynamics and control of the overall Bifocal Relay Mirror Spacecraft during the engagement operational phase, in order to validate different control options and compare their performances. Beyond the dynamics and control of the spacecraft attitude, the dynamics and control of the two fast steering mirrors, constituting the tertiary mirrors of the transmitter and receiver telescopes, is taken in account.

Section two of this paper introduces the dynamic model of the Bifocal Relay Mirror spacecraft. Section three describes the studied control approaches. The implementation of the simulation program is described in section four. Finally, the results of the numerical simulations are reported in section five.

II Dynamics of the Bifocal Relay Mirror system

A Model of the spacecraft

The Bifocal Relay Mirror Spacecraft consists of two main bodies: transmitter telescope and receiver telescope. The receiver telescope rotates with respect to the transmitter around an axis, that contains, as a design hypothesis, the center of mass of the receiver telescope itself: then the center of mass of the overall system does not change during the relative rotation of the two telescopes. Looking at figure 1 the relative rotation axis is x_R, while the center of mass of the receiver and of the overall system are respectively O_R and O_S.

The other bodies considered in the dynamic model are:

- four reaction wheels mounted in tetrahedral configuration on the transmitter telescope sec-

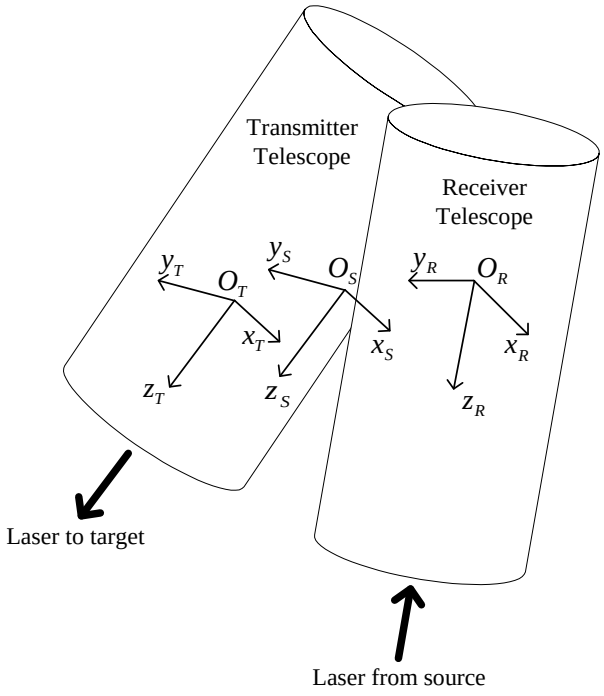

Fig. 1 High level model of the Bifocal Relay Mirror Spacecraft

tion of the system and used as actuators for the spacecraft attitude control;

- two fast steering mirrors, mounted as tertiary mirrors of the two telescopes. Each fast steering mirror is actuated in such a way it can rotates about two radial axes crossing its center of mass.

In summary, the Bifocal Relay Mirror spacecraft, as described in our model, has a total of 11 significant degrees of freedom:

- three d.o.f. for the position of the center of mass of the system;
- three d.o.f. for the attitude position of the transmitter;
- one d.o.f. for the position of the receiver with respect to the transmitter;
- two d.o.f. for the position of the transmitter fast steering mirror with respect to the transmitter;
- two d.o.f. for the position of the receiver fast steering mirror with respect to the receiver.

Let us consider the equations used to simulate the evolution of the dynamics and control of the Bifocal Relay Mirror.

A.1 Motion of the center of mass

It is derived in the simulation by propagation of the analytical solution for the circular orbit.

A.2 Attitude motion

The developed simulation program exploits the formulation of the attitude dynamics of the Bifocal Relay Mirror Spacecraft, which has been presented in ref.[3] A brief outline of the model is reported here below.

The attitude dynamics equations of the system, assumed to be composed of rigid bodies, can be written in the following vectorial form (see, for instance, ref.[4] for the underlying theory):

$$\dot{\underline{h_S}} = \underline{T_S} \tag{1}$$

where $\underline{h_S}$ and $\underline{T_S}$ are respectively the absolute total angular momentum and the total external torque about the center of mass O_S of the overall system. The time derivative on the left side of equation 1 is carried out with respect to the inertial frame.

In particular, the total angular momentum is given by the following expression:

$$\underline{h_S} = \underline{I_S}\cdot\underline{\omega} + \underline{I_R}\cdot\underline{\omega_{rel}} + \sum_{i=1}^{4} \underline{I_{w_i}}\cdot\underline{\omega_{rel_{wi}}} + \sum_{k=1}^{2} \underline{I_{m_k}}\cdot\underline{\omega_{rel_{mk}}} \tag{2}$$

where $\underline{I_S}$ and $\underline{I_R}$ are the moments of inertia dyadics respectively of the overall spacecraft and of the receiver about their respective centers of mass; $\underline{I_{w_i}}$ is the moment of inertia dyadic of the i^{th} reaction wheel about its center of mass, $\underline{I_{m_k}}$ is the moment of inertia dyadic of the k^{th} mirrors about its center of mass. Moreover $\underline{\omega}$ is the absolute angular velocity of the transmitter telescope, $\underline{\omega_{rel}} = \underline{\omega_R} - \underline{\omega}$ is the relative angular velocity of the receiver with respect to the transmitter; $\underline{\omega_{rel_{wi}}}$ is the relative angular velocity of the i^{th} reaction wheel with respect to the transmitter telescope and $\underline{\omega_{rel_{mk}}}$ is the relative angular velocity of the k^{th} mirrors with respect to its base.

In particular, the fourth term on the right of the equation 2 gives the effect of the motion of the fast steering mirrors on the dynamics of the spacecraft.

Developing the vectorial equation 2, expressing the vectors and dyadics in the same reference frame (we used the frame x_S, y_S, z_S in figure 1) and choosing a set of attitude parameters (we used the Euler parameters) three differential scalar equations, describing the attitude motion of the transmitter portion of the spacecraft, are finally obtained.

A.3 Motion of the receiver telescope with respect to the transmitter telescope

This motion is considered to follow the precomputed reference angular motion, designed in order to maintain the optical link between source and target during an orbital passage.

A.4 Motion of the fast steering mirrors with respect to their base

Typically, a fast steering is actuated by four voice-coil actuators. These are mounted behind the mirror in a cross configuration parallel to the two rotation axes. The voice coils are utilized in push-pull pairs in order to produce two orthogonal rotations. Then the mirror pivots around its center, as if it was mounted on a gimbal joint.

Each fast steering mirror is here modelled as a rigid body connected to the spacecraft by a series of two hinges, located at the center of mass of the mirror and each possessing torsional stiffness and torsional damping.

With the hypothesis of considering small relative rotation angles, each fast steering mirror is modelled as a set of two decoupled linear torsional oscillators.

Then the equations for each of the two fast steering mirrors have the linear form:

$$\begin{aligned} \ddot{\beta}_{x_m} + 2\,\xi_{x_m}\,\omega_{n_{x_m}}\,\dot{\beta}_{x_m} + \omega^2_{n_{x_m}}\,\beta_{x_m} = \\ \frac{t_{x_m}}{j_{x_m}} - \dot{\underline{\omega}} \cdot \underline{i_{x_m}} \\ \ddot{\beta}_{y_m} + 2\,\xi_{y_m}\,\omega_{n_{y_m}}\,\dot{\beta}_{y_m} + \omega^2_{n_{y_m}}\,\beta_{y_m} = \\ \frac{t_{y_m}}{j_{y_m}} - \dot{\underline{\omega}} \cdot \underline{i_{y_m}} \end{aligned} \tag{3}$$

where β_{x_m} and β_{y_m} are the relative angles of rotation of the mirror with respect to its base, around the axes x_m and y_m; ξ are the damping ratios, ω_n the natural frequencies, t the torques applied on the mirror, j the moments of inertia of the mirror. Finally, the last terms on the right of equations 3 give the component of the absolute angular acceleration of the base of the mirror along the two mirror axes, which are identified by their versors $\underline{i_{x_m}}$ and $\underline{i_{y_m}}$.

B Model of the Environmental Torques

As external disturbance torques, the gravity gradient and magnetic disturbance are considered in the model.

C Model of the Inertial Reference Unit sensors

Rate gyros to determine spacecraft angular rates and star trackers to determine spacecraft attitude

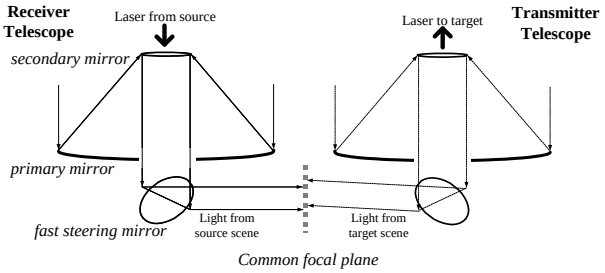

a) High level scheme of the optical subsystem

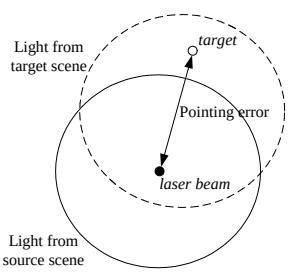

b) Images on the common focal plane: pointing error

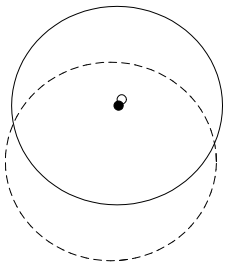

c) Compensated pointing error

Fig. 2 Basic concepts of the optical subsystem of the Bifocal Relay Mirror Spacecraft

are considered in the model. The rate gyros's bias errors and star trackers' measurement gaps have been simulated.

During the measurement gap for the star trackers, rate gyros are used to determine angular rates and angular position. When the star trackers measurements are taken, using a simulated Kalman Filter, the angular position is corrected and rate gyro biases are updated.

D Model of the optical subsystem

Figure 2(a) gives a high-level description of the optical subsystem of the Bifocal Relay Mirror spacecraft, as it has been considered for the present study. This is a basic model of the working concept: the fast steering mirrors of the transmitter and receiver telescopes convey the light respectively from the target scene and the source scene toward a common focal plane.

Figure 2(b) shows a typical situation at the beginning of the pointing process, looking on the common focal plane. While the laser beam is approximately in the center of the image from the source, which is the nominal situation, there is a pointing error between laser beam and target. By suitably moving the transmitter fast steering mirror, the image of the target moves on the common focal plane with respect to the image of the source and the error be-

tween the laser beam and the target is reduced, as figure 2(c) shows.

Several effects are present in reality, which are not considered in our preliminary optical model: in particular the jitter due to presence of atmosphere and to the structural vibrations of the spacecraft, the need of a pointing-ahead angle due to the combination of the effects of the finite propagation time of the light across the link and the relative motion of the spacecraft with respect to source and target.

Two optical tracker sensors, supposed fixed with respect to the common focal plane, process the images from the two telescopes, and their outputs are available to the controllers of the fast steering mirrors. In particular the source optical tracker senses the motion of the source beam relative to the focal plane and commands the tilting of the fast steering mirror of the receiver telescope, in order to maintain the laser beam nominally in a fixed point of the focal plane. That point corresponds to the center of the target sensor. At the same time the target optical tracker senses the motion of the target relative to the focal plane and commands the fast steering mirror of the transmitter telescope in order to reduce the pointing error.

For the study presented in this article, we focused on the control of the transmitter portion of the optical subsystem, considering the receiver portion always working nominally and maintaining the laser beam in the center of the tracker sensor. This simplifying hypothesis is based on the fact that the tracking and pointing of the source is intrinsically less demanding than the tracking and pointing of the target, because the source is supposed to be cooperative. Then, for a first characterization of the possible system performance, we concentrated our effort in simulating more realistically the target tracking and pointing. Nevertheless, we included both the receiver and the transmitter fast steering mirrors in our dynamics model.

III Control approaches

The two control approaches, described in the following subsections, have been considered in the simulations:

A Independent control of fast steering mirrors and spacecraft attitude

Using this approach, the spacecraft attitude is controlled independently of the fast steering mirrors motion. While the spacecraft attitude is controlled by feed-forward and PD commands, sensing the attitude error with the IRU, the transmitter and receiver fast steering mirrors are controlled by a PID control,

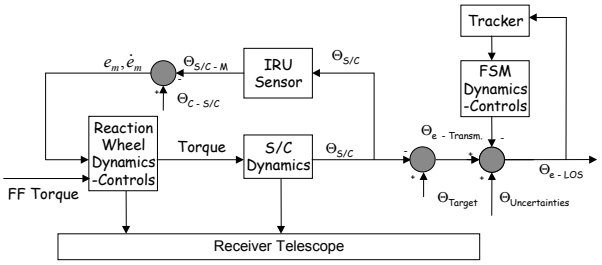

a) Independent spacecraft-fast steering mirrors control

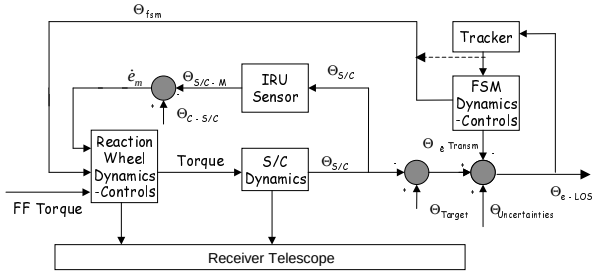

b) Integrated spacecraft-fast steering mirrors control

Fig. 3 The two control approaches considered

sensing the target and source errors with the optical sensors. This control approach is described by the block diagram in figure 3(a), with the following significance of the symbols:

- $\Theta_{S/C}$ is the true attitude of the spacecraft. In the reality this quantity is not known directly. In the simulations it is given by the integration of the equations of motion;
- $\Theta_{S/C-M}$ is the measured attitude of the spacecraft;
- $\Theta_{C-S/C}$ is the reference attitude of the spacecraft;
- Θ_{Target} is the attitude of the spacecraft at which the transmitter telescope axis hits the target. In the presented simulations this quantity is considered equal to $\Theta_{C-S/C}$;
- $\Theta_{e-transm} = \Theta_{Target} - \Theta_{S/C}$ is the pointing error;
- $\Theta_{uncertainties}$, the line of sight uncertainties. They can derive from different causes: motion of the target, imperfect knowledge of the reference attitude, LOS jitter. In some of the presented simulations (defined as simulations with target in uncertain position), we considered uncertainties given by a low frequency pseudo-random signal, as later on explained;
- Θ_{e-LOS} is the total pointing error, including the uncertainties and the correction from the fast steering mirror.

B Integrated control of transmitter fast steering mirror and spacecraft attitude

Using this control approach, the transmitter fast steering mirror position relative to the structure is measured and used to control the spacecraft attitude. Indeed, the mirror position is proportional to the not corrected target pointing error. The angular position around the yaw axes and the angular rate data, for the attitude control, still comes from the IRU sensors. As regards the receiver fast steering mirror, it is still considered controlled independently. The concept of this control approach is described by the block diagram in figure 3(b). The dashed line on the output of the target tracker indicates that, in the simulation with fixed fast steering mirror, we considered directly the output of the target as a feedback signal.

IV Implementation of the simulation program

The system dynamics and control laws described above has been implemented in a simulation program coded in MATLAB/SIMULINK, using as a base the software described in ref.[3]

The main simplifying hypotheses, considered in the development of the model, are summarized here below:

1. The error between the correct attitude and the actual attitude is considered small, in order to apply the simplifications of small angles in the related attitude kinematics equations and in order to model as two decoupled second order systems the dynamics of each fast steering mirror around its two axes;
2. The relative motion between transmitter and receiver telescope is considered following the reference relative motion without error;
3. The target and source tracker sensors are considered ideal, giving continuous output;
4. The beam jitter has not been modelled;
5. The reference attitude profile was chosen similar to a typical slewing maneuver for the Bifocal Relay Mirror, without a detailed design of the maneuver.

While the first hypothesis will maintain its validity in the real operational life of the Bifocal Relay Mirror, at least during the acquisition mode phases, the other hypotheses are considered helpful in the preliminary study carried out.

The following two different sample cases were studied in the simulations:

1. Target and source in certain position: in this case the position of target and source is considered perfectly known a priori ($\Theta_{uncertainties} = 0$). The design of the reference attitude motion is based on that knowledge. Therefore, in principle, the spacecraft attitude motion along that reference motion, guarantees a perfect alignment of the laser beam both with the source and target. This is an ideal condition, useful to evaluate the maximum achievable performance. The target and source trackers sense the relative pointing errors between the target or source and the laser beam spots. In the simulations, the computation of the relative pointing error is based on the knowledge of the exact attitude of the spacecraft, obtained by the integration of the spacecraft dynamics.

2. Target in uncertain position: in this more realistic case the position of the target is not considered perfectly known a priori ($\Theta_{uncertainties} \neq 0$). Such uncertainty can derive by different causes, as the imperfect knowledge of the orbital trajectory of the spacecraft, the motion of the target with respect to the background scene, and the LOS jitter. The uncertainty in the target position has been modelled in the simulation program by adding pseudo-random signals to the target relative pointing error, output by the target sensor. The pseudo-random signals were obtained by low pass filtering the output of a white noise signal. On the contrary, the source position is still considered perfectly known.

V Simulation results

A Value of the main simulation parameters

A.1 Integration parameters

The simulation time period is $500\,seconds$. The simulation solver method is ode5 (Dormand-Prince), and the solver fixed step size is $0.005\,seconds$.

A.2 Dynamics parameters

Altitude of the circular orbit: $715\,Km$. Mass of the transmitter telescope: $m_1 = 2267\,Kg$, mass of the receiver telescope: $m_2 = 972\,Kg$. Transmit telescope inertia: $I_{x_T x_T} = 2997\,Kg\,m^2$, $I_{y_T y_T} = 3164\,Kg\,m^2$, and $I_{z_T z_T} = 882\,Kg\,m^2$; receiver telescope inertia: $I_{x_R x_R} = 1721\,Kg\,m^2$, $I_{y_R y_R} = 1560\,Kg\,m^2$, and $I_{z_R z_R} = 183\,Kg\,m^2$. For both the transmitter and receiver fast steering mirrors: $j_{x_m} = j_{y_m} = 0.01\,Kg\,m^2$. Natural frequency around both x and y axes: $\omega_{n_{x_m}} = \omega_{n_{y_m}} = 10\,Hz$. Damping ratio around both x and y axes $\xi_{x_m} = \xi_{y_m} = 0.01$.

A.3 Optical parameters

Magnification factor of both telescopes: 8.2. Field of view for both telescopes: $5\,e^{-4}\,rad$. This field of view corresponds to a circular footprint area with radius of $375\,m$ on the earth surface, when the telescope axis is perpendicular to the surface.

A.4 Disturbance parameters

The secular torques magnitude is $1\,e^{-4}\,Nm$. The control law delay for initial determination errors is $30\,seconds$. A star tracker measurement gap is considered in the period between 100 and $300\,seconds$. The rate gyros static rate biases are $1\,e^{-4}\,[-1, 1.5, 1]\,rad/sec$. The initial errors are set: for quaternion $[0.008, 0.012, -0.008]$ and for angular rate $[-0.001, 0.001, 0.002]\,rad/sec$. Control gains for the PD control of the spacecraft, $k = [1500, 3500, 2250]$ and $k_d = [1000, 2000, 1000]$. For the reaction wheels, the maximum allowable torque is $1\,Nm$ and the maximum angular momentum is $10\,Nm/sec$. Gains for the PID control of the transmitter fast steering mirrors: $k = [160, 160]$, $k_d = [10, 10]$, $k_i = [15, 15]$.

B Reference attitude motion of the spacecraft

The profile of the reference attitude motion is shown in figures 4. The profile resembles the maneuver required to maintain transmitter and receiver telescopes pointing the source and target during an overhead pass to conduct laser relay operations. The majority of the maneuver is performed in the spacecraft pitch axis, q_2, as both telescopes orient to point at fixed ground sites. The largest relative angle, that in reality is based on the ground site location of target and source, is considered about $30\,degrees$ during a near overhead pass.

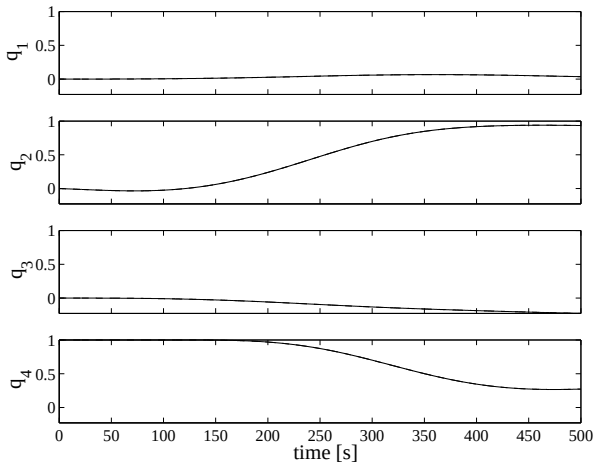

a) Transmitter telescope reference rotation in quaternions

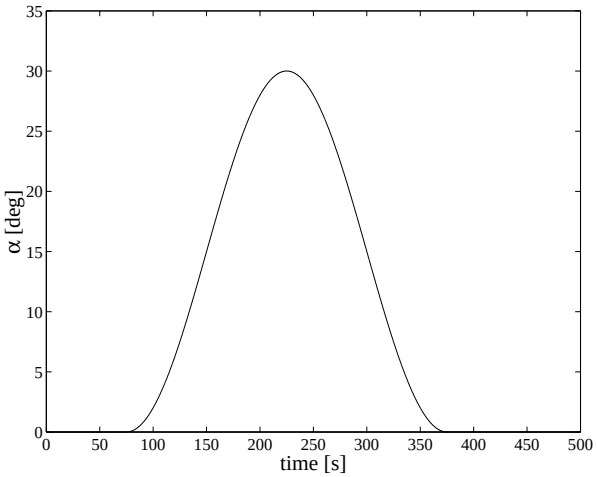

b) Relative rotation angle of the receiver telescope with respect to the transmitter

Fig. 4 The reference motion of the spacecraft

C Outline of the results

The independent and integrated control approaches, described in paragraph III, were applied to both the cases with certain and uncertain knowledge of the target position, described in paragraph IV. This combination of tests has been carried out with the following two configurations of the system:

1. Ideal IRU sensors output, continuously available; this constitutes a reference case;

2. Realistic IRU sensors output and Kalman filter.

Figures 5 report the pseudo-random signals added to the target sensor output, during the simulations with uncertain knowledge of the target position. In particular, Figure 5(b) gives the simulated view of the target track relative to the common focal plane, looking through the telescope. In other words that is the simulated view of the target as captured by the target tracker sensor. The laser beam spot from the source on the common focal plane corresponds to the center of the square area in the figures and each side of the square corresponds to the field of view of the telescope. This kind of figure was considered the most effective method of representing the results in the following.

Figures 6 and 7 represent the results of the simulations in the case of system with ideal IRU. The results are represented after the initial 30 seconds, during which the attitude control is switched off, while the initial determination is carried out. The case of uncontrolled target error (i.e. mirror fixed) is compared to the case of target error controlled by tilting the fast steering mirror. Moreover the case of independent spacecraft-fast steering mirrors control

is compared to the case of integrated spacecraft-transmitter fast steering mirror control. For the simulations of figures 7 the position of the target was considered uncertain, with the meaning specified in paragraph IV.

Figures 8 and 9 represent the results of the simulations in the case of system with realistic IRU sensors and Kalman filter. For the simulations in figures 9 the position of the target was considered uncertain.

Figures 10 represent the time history of the track error, for the case in figures 9. The picks in the error around 300 seconds, in figure 10(a), are due to the end of the measurement gap in the star tracker.

In the simulations with ideal sensors and uncertainties in the target position (figures 7), the integrated control worsens the performance with respect to the independent control. On the contrary in the case of realistic IRU sensors (figures 9), the integrated control improves the performance with respect to the independent control. An explanation for these facts is that in both cases the target sensor is considered ideal and giving continuous reading. The uncertainties are added to the ideal output of the target sensor. Then, while in the first case the target sensor output does not improve the reading of the IRU sensor, but spoils that reading because of the added uncertainties, in the second case it does improve the reading of the IRU sensor, that is affected by the biases of the rate gyros.

VI Conclusions

Simulations have been carried out on a dynamics model of the Bifocal Relay Mirror Spacecraft in order to preliminary validate and compare two different proposed control approaches. In particular, an independent control of fast steering mirrors and spacecraft attitude and an integrated control of transmitter fast steering mirror and spacecraft attitude have been investigated.

Based on the results obtained in the simulations, it appears that the best solution to control the Bifocal Relay Mirror system is probably a trade-off between the independent spacecraft-fast steering mirrors control and the integrated spacecraft-transmitter fast steering mirror control. That is a control that uses a fusion of the data from the target and source tracking sensors and the data from the IRU sensors, weighted on the base of the knowledge of the characteristics of the specific sensors.

Further studies can be carried out by developing the dynamics model and the simulation program in order to overcome the hypotheses taken in account in the present study and summarized in paragraph IV.

Aknowledgment

This work was carried out while Dr.Marcello Romano was holding a National Research Council Research Associateship Award at the Spacecraft Research and Design Center.

The work of Lt.Chris Senenko on a previous version of the simulation software is gratefully acknowledged.

References

[1]G.Baister and P.V.Gatenby, "Pointing, acquisition and tracking for optical space communications," *electronics and communication engineering journal*, vol. 6, pp. 271–280, December 1994.

[2]J.F.Sullivan, J.E.Anspach, and P.W.Kervin, "Relay mirror experiment and wideband angular vibration experiment," program summary, Ball Aerospace Systems Group, 1992.

[3]B. Agrawal and C. Senenko, "Attitude dynamics and control of bifocal relay mirror spacecraft," in *AAS/AIAA Astrodynamics Specialists Conference*, (AAS Paper 01-418, Quebec City, Canada), August 2001.

[4]P.C.Hughes, *Spacecraft attitude dynamics*. New York: John Wiley & Sons, 1986.

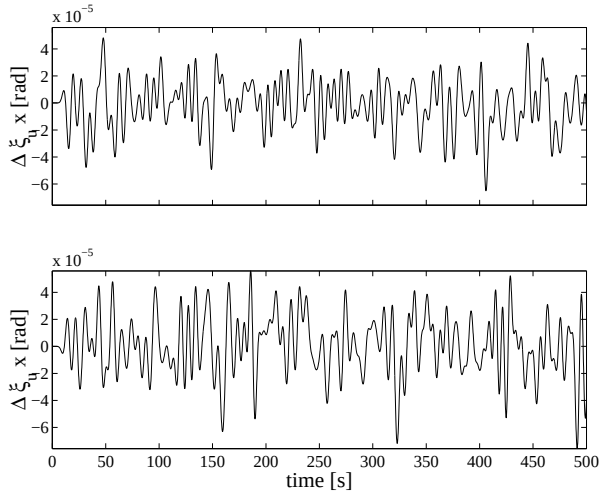

a) Pseudo-random signals over time

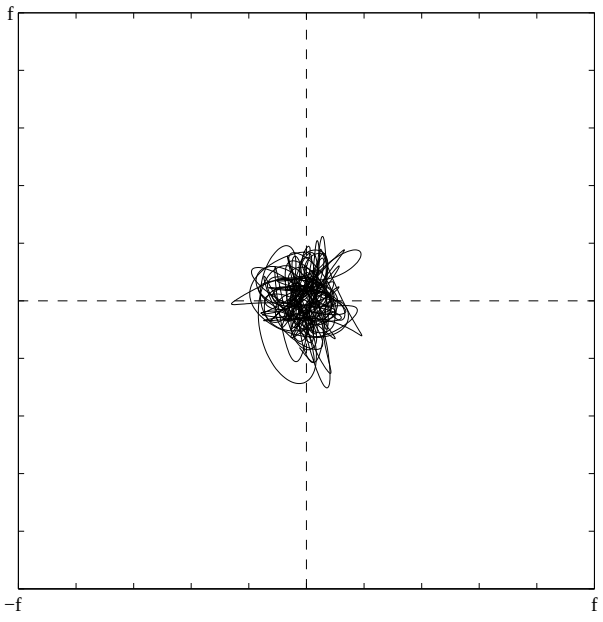

b) Simulated view of the target track relative to the common focal plane

Fig. 5 Pseudo-random signals added to the target sensor output, during the simulations with uncertain knowledge of the target position.

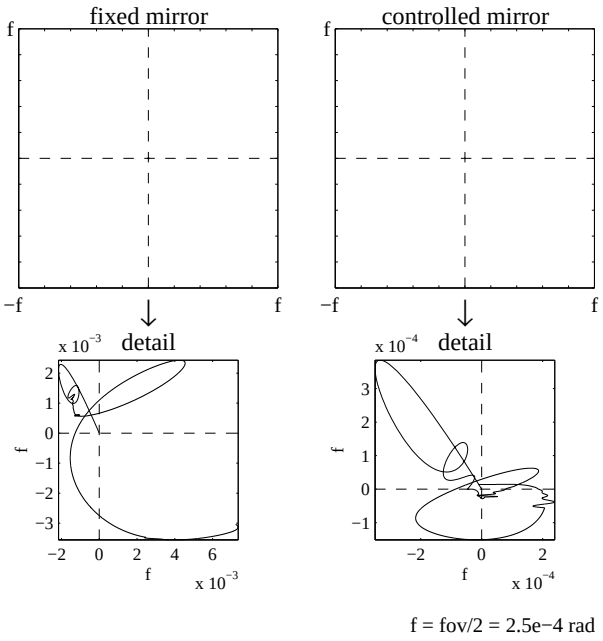

a) Case with independent spacecraft-fast steering mirror control

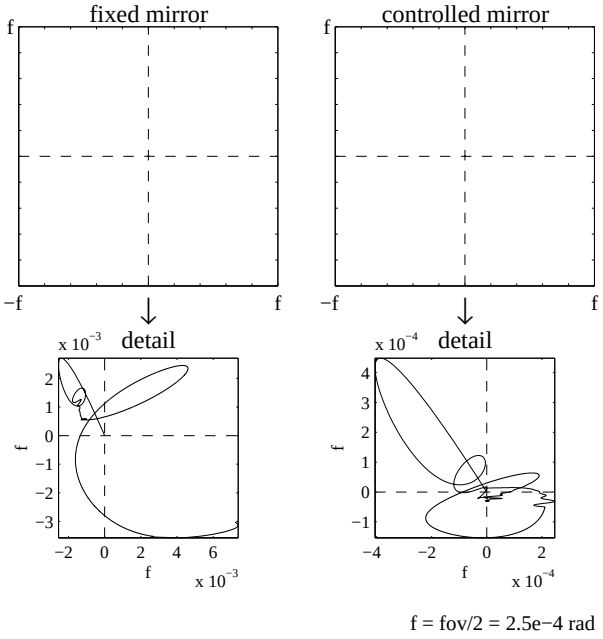

b) Case with integrated spacecraft-transmitter fast steering mirror control.

Fig. 6 Simulated view of the track of the target on the target sensor: spacecraft with ideal IRU and certain knowledge of the target position.

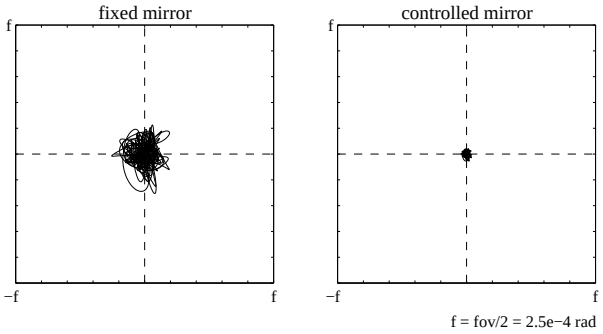

a) Case with independent spacecraft-fast steering mirror control

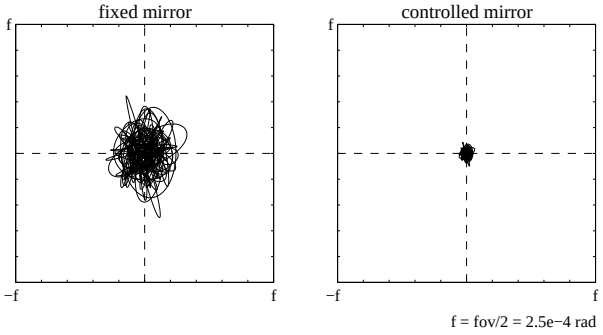

b) Case with integrated spacecraft-transmitter fast steering mirror control.

Fig. 7 Simulated view of the track of the target on the target sensor: spacecraft with ideal IRU and uncertain knowledge of the target position.

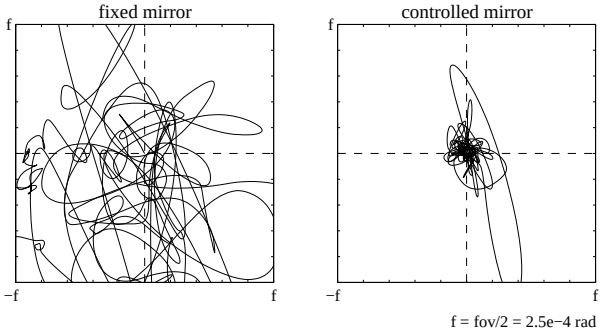

a) Case with independent spacecraft-fast steering mirror control

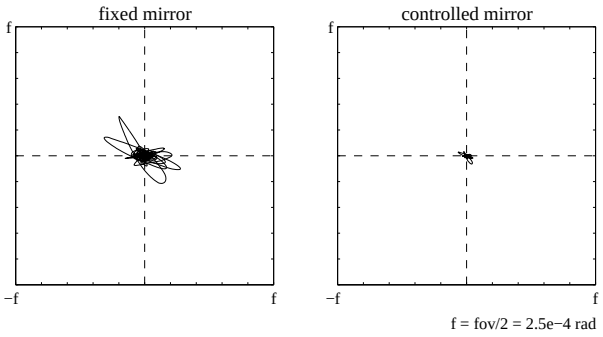

b) Case with integrated spacecraft-transmitter fast steering mirror control.

Fig. 8 Simulated view of the track of the target on the target sensor: spacecraft with realistic IRU and Kalman filter, and certain knowledge of the target position.

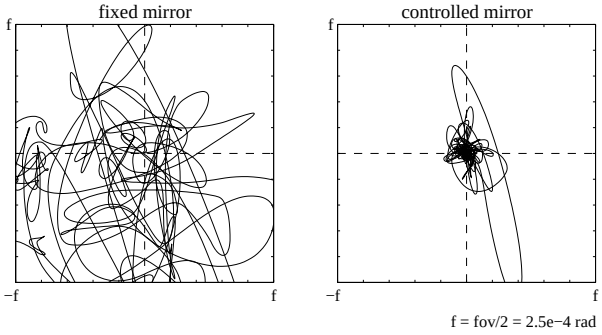

a) Case with independent spacecraft-fast steering mirror control

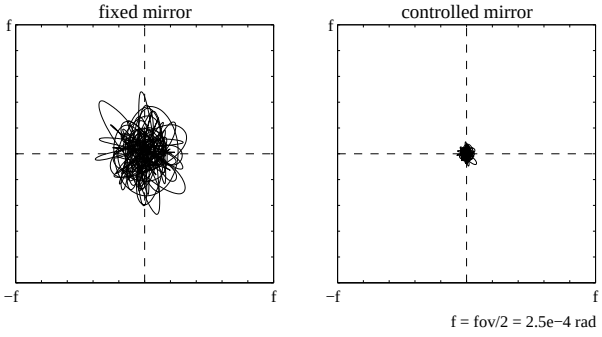

b) Case with integrated spacecraft-transmitter fast steering mirror control.

Fig. 9 Simulated view of the track of the target on the target sensor: spacecraft with realistic IRU and Kalman filter, and uncertain knowledge of the target position.

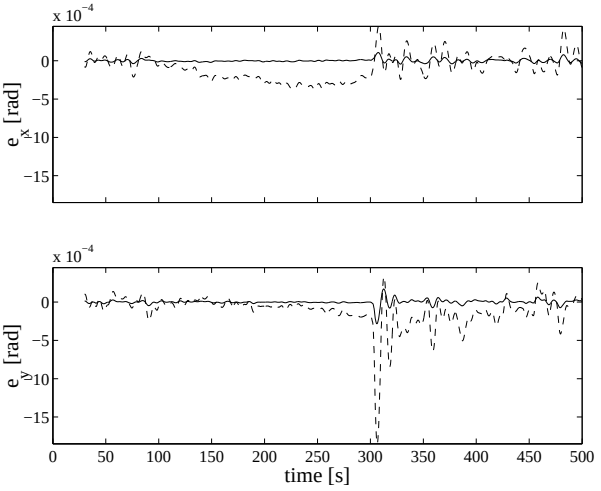

a) Case with independent spacecraft-fast steering mirror control

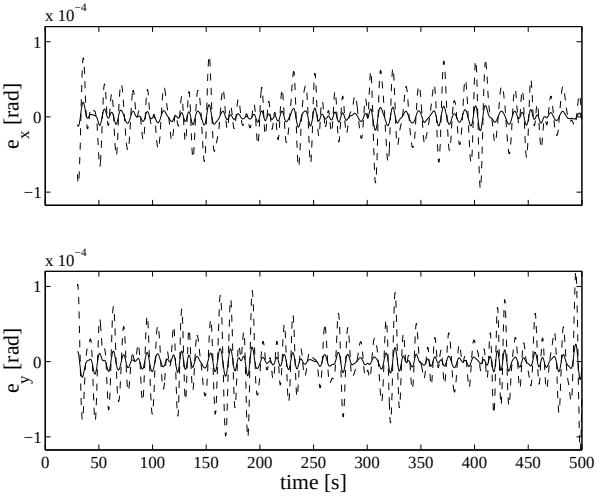

b) Case with integrated spacecraft-transmitter fast steering mirror control.

Fig. 10 Track error history vs time. Spacecraft with realistic IRU and Kalman filter, and uncertain knowledge of the target position.